

Bragg-induced oscillations in non- \mathcal{PT} photonic lattices

P. A. Brandão^{a,*}, S. B. Cavalcanti^a

^a*Universidade Federal de Alagoas, Instituto de Física, Cidade Universitária, Maceió-AL, 57072-970, Brazil*

Abstract

When a monochromatic beam of light propagates through a periodic structure with the incident angle satisfying the Bragg condition, its Fourier spatial spectra oscillates between the resonant modes situated on the edges of the Brillouin zones of the lattice with a nontrivial dynamics. We wish to study here these Bragg-induced oscillations in a specific non- \mathcal{PT} periodic structure, that is, a periodic medium not invariant under the combined action of parity and time reversal symmetries. We compare our analytic results based on the expansion of the optical field in Bragg-resonant plane waves with direct numerical integration of the paraxial wave equation using a wide Gaussian beam as initial condition without assuming the shallow potential approximation. In particular, we wish to investigate under what conditions a mode trapping phenomenon can still be observed and to verify closely how the energy exchange between the spectral modes takes place during propagation in this more general class of potentials with arbitrary gain and loss profiles.

Keywords: Bragg resonance, Parity-Time symmetry, Paraxial propagation

1. Introduction

The unified concept of Parity-Time (\mathcal{PT}) symmetry introduced by Bender and Boettcher almost 20 years ago is now part of an active area of scientific research [1, 2, 3, 4]. Systems that are invariant under the combined action of parity and time symmetries can be described by non-Hermitian operators that possess a real-valued spectra. An operator (a Hamiltonian H , for instance) is said to be \mathcal{PT} -symmetric if it commutes with the \mathcal{PT} operator, $[\mathcal{PT}, H] = 0$. However, this condition alone does not guarantee that both commuting operators will share a common set of eigenvectors because the operator \mathcal{T} is antilinear. In practice, the Hamiltonian $H(b)$ contains a free parameter b that can be tuned arbitrarily and, depending on its value, the Hamiltonian can have its symmetry spontaneously broken. When the symmetry of the Hamiltonian is broken, even though it commutes with \mathcal{PT} , they do not share a common set of eigenvectors and its eigenvalues can become completely or partially complex. In the physical context, \mathcal{PT} symmetry behavior has been experimentally demonstrated in

*Corresponding author

Email address: paulocabf@mail.com (P. A. Brandão)

optical coupled waveguides [5, 6, 7], Silicon photonic circuits [8], superconducting wires [9] and even in classical mechanical systems [10], to cite a few.

Even though the concept of \mathcal{PT} symmetry has increased the class of possible physical Hamiltonians, by extending Hermitian systems to the complex plane, such required symmetry is not sufficient or necessary for an operator to possess a real-valued spectra. Although it can be shown that the eigenvalues of a \mathcal{PT} -symmetric Hamiltonian will always come as complex-conjugate pairs, this property is not exclusive to the \mathcal{PT} symmetry. A necessary and sufficient condition for the spectrum of a non-Hermitian Hamiltonian to be purely real can be formulated in terms of a more general class of pseudo-Hermitian operators. It was shown extensively by Mostafazadeh, shortly after the seminal work of Bender and Boettcher, that Hamiltonians with \mathcal{PT} symmetry are actually a subgroup of a more general class of pseudo-Hermitian Hamiltonians [11, 12, 13, 14]. In this theory, an operator H is said to be η -pseudo-Hermitian if there exists a Hermitian invertible linear operator η such that $H^\dagger = \eta H \eta^{-1}$. It was shown recently that it is possible to consider a looser set of conditions on the pseudo-Hermiticity by requiring η not to be invertible [15]. We will discuss this new class of operators in section 2 below.

Optical beam oscillations induced by Bragg-resonance were studied ten years ago by Shchesnovich and Chávez-Cerda assuming a shallow potential approximation [16]. The periodic exchange of spectral energy between two considered modes resemble the old Rabi problem, where oscillations between quantum states is present in two-level systems, and the authors called this Bragg-induced oscillation Rabi oscillations as well. However, we find more transparent and unambiguous to call these Bragg-induced oscillations simply Bragg oscillations. This is because there are other types of Rabi-like oscillations present in photonic systems [17, 18, 19]. Bloch oscillations in an optical setup with \mathcal{PT} symmetry was also considered [20]. Until now, attention to Bragg oscillations in optical beams propagating in periodic photonic structures was devoted to linear and Hermitian [16], linear and \mathcal{PT} -symmetric [21] and nonlinear and Hermitian structures [22]. In this paper, we consider Bragg oscillations in a more general class of potentials and show that new effects and unexpected results are present when the optical medium no longer has \mathcal{PT} symmetry.

Section 2 is devoted to a discussion of non- \mathcal{PT} potential operators and its spectra, where we show explicitly how one can construct such potentials. We also introduce the periodic potential that is used throughout the paper. Section 3 presents the evolution equations for the spectral amplitudes of individual resonant plane waves as a first order coupled system of differential equations. This system is solved by numerical techniques in section 4 along with its physical interpretation. Our conclusions are presented in section 5.

2. Non- \mathcal{PT} Hamiltonians

As pointed out in the last section, new classes of general non- \mathcal{PT} symmetric potentials with arbitrary gain and loss regions were introduced [23, 24, 25, 26, 15]. This is a huge step forward in the ability to construct arbitrary complex materials while still preserving a real spectrum of eigenvalues. We follow one such specific method for constructing arbitrary classes of complex materials that was introduced very recently [15]. If $L = d^2/dx^2 + V(x)$ is

a Schrödinger operator and if there exists another operator η such that L and η are related by a similarity relation

$$\eta L = L^* \eta, \quad (1)$$

then it is easy to show that all eigenvalues of L come in conjugate pairs if the kernel of η is empty [26]. This resemble the approach developed by Mostafazadeh [11, 12] but, in the present situation, η need not be invertible. Given the generality of the η operator, we choose it to be a combination of the parity operator \mathcal{P} and differential operators as in

$$\eta = \mathcal{P} \left[\frac{d}{dx} + h(x) \right], \quad (2)$$

where $h(x)$ is an complex function whose properties we will now derive. When the right hand side of (1) acts on an arbitrary function $g(x)$ we have

$$\begin{aligned} L^* \eta g(x) &= \left[\frac{d^2}{dx^2} + V^*(x) \right] \mathcal{P} \left[\frac{dg(x)}{dx} + h(x)g(x) \right] \\ &= \left[\frac{d^2}{dx^2} + V^*(x) \right] \left[-\frac{dg(-x)}{dx} + h(-x)g(-x) \right] \\ &= -\frac{d^3 g(-x)}{dx^3} + \frac{d^2 [h(-x)g(-x)]}{dx^2} - V^*(x) \frac{dg(-x)}{dx} + V^*(x) h(-x)g(-x), \end{aligned} \quad (3)$$

while the left hand side of (1) reads

$$\begin{aligned} \eta L g(x) &= \mathcal{P} \left[\frac{d}{dx} + h(x) \right] \left[\frac{d^2 g(x)}{dx^2} + V(x)g(x) \right] \\ &= \mathcal{P} \left[\frac{d}{dx} + h(x) \right] \left[\frac{d^2 g(x)}{dx^2} + V(x)g(x) \right] \\ &= -\frac{d^3 g(-x)}{dx^3} - \frac{d[V(-x)g(-x)]}{dx} + h(-x) \frac{d^2 g(-x)}{dx^2} + h(-x)V(-x)g(-x). \end{aligned} \quad (4)$$

Since (1) must be satisfied,

$$\begin{aligned} \frac{d^2 [h(-x)g(-x)]}{dx^2} - V^*(x) \frac{dg(-x)}{dx} + V^*(x) h(-x)g(-x) = \\ - \frac{d[V(-x)g(-x)]}{dx} + h(-x) \frac{d^2 g(-x)}{dx^2} + h(-x)V(-x)g(-x), \end{aligned} \quad (5)$$

and, after letting $x \rightarrow -x$ and setting all coefficients of $g(x)$ and $dg(x)/dx$ equal to zero (because $\eta L - L^* \eta$ is the null operator), we have the following coupled differential equations

$$V(x) - V^*(-x) = 2 \frac{dh(x)}{dx}, \quad (6)$$

and

$$[V(x) - V^*(-x)]h(x) = \frac{d^2 h(x)}{dx^2} - \frac{dV(x)}{dx}. \quad (7)$$

After taking the complex conjugate of (6) together with the substitution $x \rightarrow -x$, it is easy to see that

$$-\frac{dh^*(-x)}{dx} = \frac{1}{2}[V^*(-x) - V(x)] = -\frac{dh(x)}{dx}, \quad (8)$$

which follows that $dh^*(-x)/dx = dh(x)/dx$ and, after integrating both sides, $h^*(-x) = h(x) + c_1$ with c_1 being the constant of integration. Next, let us substitute the right hand side of (6) into the left hand side of (7) to obtain

$$2h(x)\frac{dh(x)}{dx} = \frac{d^2h(x)}{dx^2} - \frac{dV(x)}{dx}, \quad (9)$$

and, after integrating once,

$$\int^{h(x)} 2h dh = \int^{\frac{dh}{dx}} d\left(\frac{dh}{dx'}\right) - \int^{V(x)} dV + c_2, \quad (10)$$

where c_2 groups all constants of integration. It is then easy to see that $V(x)$ is given by

$$V(x) = \frac{dh(x)}{dx} - h^2(x) + c_2. \quad (11)$$

Since c_2 only adds a constant value to the potential function, we can, without loss of generality, take it as $c_2 = 0$. To find the value of c_1 we substitute (11) and the expression $h^*(-x) = h(x) + c_1$ into (6)

$$c_1[2h(x) + c_1] = 0. \quad (12)$$

Therefore, we can choose $c_1 = 0$. Since now $h^*(-x) = h(x)$ it follows that the function $h(x)$ is \mathcal{PT} -symmetric. So, by choosing a function $h(x)$ \mathcal{PT} -invariant we can generate the potential function

$$V(x) = \frac{dh(x)}{dx} - h^2(x). \quad (13)$$

The choice of the \mathcal{PT} -symmetric $h(x)$ function is completely arbitrary and, in order to study a periodic potential, we follow [15] in choosing $h(x) = 1 + \cos x + ib \sin x$, which clearly has the desired symmetry, and b is a positive free real and positive parameter. The potential is given explicitly by

$$V(x) = b^2 \sin^2 x - \cos^2 x - \sin x - 2 \cos x - 1 + ib[\cos x - 2 \sin x - \sin(2x)], \quad (14)$$

where one can clearly see that the imaginary part is not odd, the real part of the potential is not even and this periodic potential has period 2π . Nevertheless, the spectrum of (14) is completely real for $b < 1$ and partially complex for $b > 1$ as shown in [15]. Therefore, this is an explicit example of a potential that is not \mathcal{PT} -symmetric and yet has a symmetry breaking point. In the next section we will address the problem of light propagation through a potential function as given in (14). In particular, we will be interest in the evolution of the Bragg modes when the lattice is at the symmetry breaking point $b = 1$.

3. Evolution equations

We will assume from now on that the propagation of monochromatic scalar optical beams $\psi(x, z)$ is well described by the dimensionless (1+1)-dimensional paraxial wave equation

$$i\psi_z = -\psi_{xx} + V(x)\psi, \quad (15)$$

where z is the propagation distance, x the transverse coordinate and $V(x)$ is the potential (14) representing the properties of the photonic lattice. Before we discuss the ansatz used to solve (15) we decompose the potential $V(x)$ into its harmonic components

$$V(x) = \sum_{n=-\infty}^{\infty} V_n e^{inx} = V_{-2}e^{-2ix} + V_{-1}e^{-ix} + V_0 + V_1e^{ix} + V_2e^{2ix}, \quad (16)$$

where the, generally complex, Fourier amplitudes of the potential are given by $V_{-2} = -(1/4)(1-b)^2$, $V_{-1} = -(i/2 + 1)(1-b)$, $V_0 = -[1 + (1-b^2)/2]$, $V_1 = (i/2 - 1)(1+b)$ and $V_2 = -(1/4)(1+b)^2$. The fact that some Fourier amplitudes are complex numbers is a clear signature of the non- \mathcal{PT} nature of the potential. That this must be so follows from the fact that, if the potential is \mathcal{PT} -symmetric, then, $V(x) = \sum_n V_n e^{inx} = \sum_n V_n^* e^{inx} = V^*(-x)$ which implies $V_n \in \mathbb{R}$.

Since it is known that only resonant Bragg modes are coupled during propagation when the incident beam is wide [16, 21, 22], we choose the ansatz to be

$$\psi(x, z) = \sum_{n=0, \pm 1, \pm 2, \dots} \psi_n(z) \exp(inx), \quad (17)$$

where $\psi_n(z)$ represents the spectral amplitude of mode n at a distance z . After substituting expressions (16) and (17) into the paraxial wave equation (15) we arrive at the following set of coupled first order differential equations for the spectral amplitudes $\psi_n(z)$:

$$i \frac{d\psi_n}{dz} = (n^2 + V_0)\psi_n + V_{-2}\psi_{n+2} + V_{-1}\psi_{n+1} + V_1\psi_{n-1} + V_2\psi_{n-2}. \quad (18)$$

We will also be interested in the power as a function of z , which can be calculated directly from the field $\psi(x, z)$ or as an incoherent sum of all spectral amplitudes $\psi_n(z)$:

$$P(z) = \int_{-\infty}^{\infty} |\psi(x, z)|^2 dx = \sum_{n=0, \pm 1, \pm 2, \dots} |\psi_n(z)|^2. \quad (19)$$

The second equal sign used in relation (19) is not strictly correct since plane waves have infinity energy, so the right hand side of this equation should be viewed as energy per unit (transverse) length. The general outline for the rest of the paper is to solve system (18), by considering a finite number of modes, subjected to initial conditions and to determine its power and Fourier spectra evolution.

4. Numerical results and discussion

To start, let us assume that only eleven modes are coupled through relation (18): $n \in \{\pm 5, \pm 4, \pm 3, \pm 2, \pm 1, 0\}$. With this approximation, the system (18) can be solved numerically after specifying the initial conditions on the eleven spectral amplitudes $\psi_n(0)$. Let us consider the lattice at the symmetry breaking point, $b = 1$, and that only mode $n = 0$ is initially populated, $\psi_0(0) = 1$, with all others modes empty. Figure 1 shows the power evolution, $P(z) = \sum_n |\psi_n(z)|^2$, calculated in terms of the spectral amplitudes, along with the power evolution, $P(z) = \int |\psi(x, z)|^2 dx$, calculated from the numerical solution of (15) with a Gaussian beam as initial condition, given by

$$\psi(x, 0) = \exp \left[-\frac{1}{2} \left(\frac{x}{W} \right)^2 \right], \quad (20)$$

where W is the initial beam width. Part (a) of Figure 1 depict the power evolution with $W = 10$ and parts (b) and (c) with $W = 25$ and $W = 50$, respectively. One can conclude from Figure 1 that when the initial beam width gets larger, our approximation describes very well the power evolution. This is due to the fact that the beam's width is inversely proportional to its Gaussian distribution in Fourier (reciprocal) space and, therefore, we should expect this finite-width beam approach to approximate in some sense the plane wave approach. Also, by close inspecting the profiles shown in Figure 1, one can see that the power evolution is not exactly a sine or cosine function due to the appearance of some relatively small bumps between the maximum and minimum points. Until now, no explanation or study has been given to the fundamentals of such specific behavior of the power evolution, to our knowledge. This behavior can be explained, in a more fundamental way, by examining the excited Bragg-modes of the wavefield, as we now show. Figure 2 depicts the excited Fourier modes during propagation for $\{\psi_0, \psi_1, \psi_2, \psi_3\}$. The modes with n negative are exactly zero for this particular set of parameters and the modes $n = 4, 5$ are negligible on the scale shown in Figure 1 and are therefore suppressed. Surprisingly, mode ψ_0 is trapped at $k = 0$, in the sense that its spectral energy does not change during propagation. On the other hand, the modes ψ_1, ψ_2 and ψ_3 experience oscillatory power oscillations [16, 21]. We can see now that the slightly bumps appearing in Figure 1 are due to the excited Bragg mode $n = 2$, as shown in Figure 2, something that is far from trivial after a look at the power evolution. Since only modes with $n \geq 0$ are excited in this scenario, we expect the beam to propagate in the positive direction of the x axis. This can be seen in Figure 3 where the intensity, $|\psi(x, z)|^2$, of the Gaussian beam with $W = 50$ is shown. By comparing Figures 1 and 3, it can be seen that the points of minimum value in the power evolution can be correlated to the minimum values of the intensity, as expected.

Next, we consider the spectral component $n = 1$ to be initially populated, $\psi_1(0) = 1$, and all others empty. The evolution of the spectral amplitudes ψ_1, ψ_2 and ψ_3 is shown in Figure 4(a), after numerically solving the system (18). The others eight spectral components are either zero or negligible on the scale of the plot and are, therefore, not shown. One can see that, once more, the initially populated amplitude is trapped during propagation. The initial spectral energy at $n = 1$ remains invariant. On the other hand, the Bragg modes $n = 2$

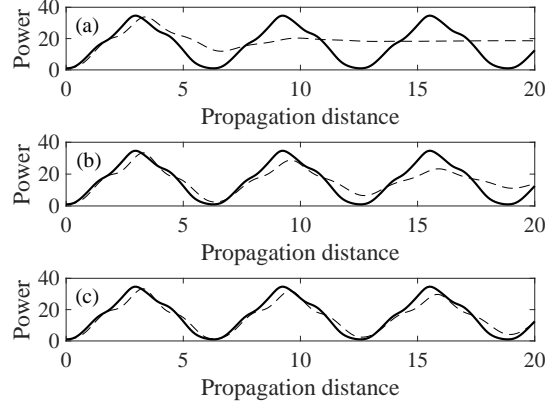


Figure 1: Power evolution in a lattice without \mathcal{PT} symmetry given by (14). Continuous lines are taken from the solutions of (18). Dashed lines are plotted from the numerical solution of the paraxial wave equation with a Gaussian input of the form $\psi(x, 0) = \exp[-(x/W)^2]$ with (a) $W = 10$, (b) $W = 25$ and (c) $W = 50$.

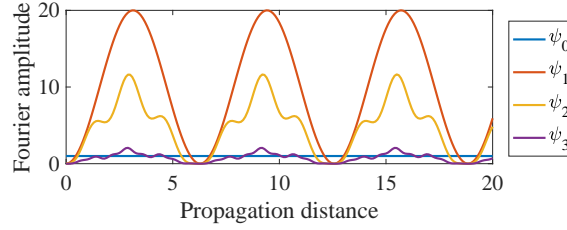


Figure 2: Evolution of the Fourier amplitudes $|\psi_n(z)|^2$ for $n = 0, 1, 2$ and 3 , corresponding to the parameters of Figure 1. The other spectral amplitudes are not shown because they are negligible compared to the ones shown. In fact, the spectral amplitudes ψ_n for $n = -5, -4, -3, -2$ and -1 are identically zero. It is easy too see that the sum of the four curves in this plot is equal to the resultant continuous curve for the power evolution shown in Figure 1. This is to be expected according to relation (19).

and $n = 3$ perform periodic Rabi-like oscillations and are therefore continuously exchanging energy with the medium. The amplitude of oscillation of mode $n = 2$ is approximately half the amplitude of mode $n = 1$. Part (b) of Figure 4 depicts the power evolution for these parameters. One can, again, clearly see a very close agreement between the model (17), represented by the continuous line, and the Gaussian beam, represented by the dashed line, which, in this case, was taken as $\psi(x, 0) = \exp[-(1/2)(x/W)^2] \exp(ix)$ to simulate the initially excited Bragg mode $n = 1$. The power oscillates in a more sinusoidal form than the previous situation presented in Figure 1. Figure 4(c) depicts the intensity evolution $|\psi(x, z)|^2$ for $W = 50$. One can see that, as only positive Bragg modes are excited, the beam has a tendency to travel to the right, as expected. Comparing the intensity evolution displayed in part (c) with the power evolution in part (b), we see that the beam absorbs much less energy from the medium compared to Figure 1. This is due to the fact that the spectral component $n = 2$ oscillates with a much smaller amplitude than the spectral component $n = 1$. This should be contrasted with the amplitude of mode $n = 1$ shown in

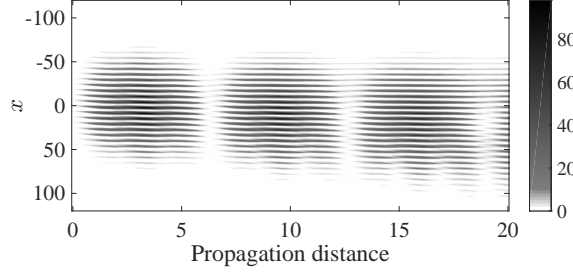


Figure 3: Intensity evolution in the (x, z) plane for a Gaussian beam propagating through the lattice (14) with $W = 50$. The regions where the intensity is a minimum are related by the power evolution of Figure 1.

Figure 2.

Now let us address one of the situations considered in [15] where the mode $n = 2$ is initially populated. Figure 5 shows the results of the numerical simulations involving plane waves and a Gaussian beam given by $\psi(x, 0) = \exp[-(1/2)(x/W)^2] \exp(2ix)$ to match the initially populated mode $n = 2$. Once more, the energy of the initially populated spectral mode is trapped, as can be seen in part (a) of Figure 5. But in this situation, besides the $n = 2$, only mode $n = 3$ contributes to the evolution of the beam by oscillating Rabi-like during propagation, as the yellow color line in Figure 5(a) shows. From previous discussions we conclude that the Bragg contributions to the power evolution are given by a constant function and an oscillatory one. Part (b) of Figure 5 shows the power evolution from the Bragg modes (continuous line) compared to the Gaussian beam power (dashed line). The agreement between the two approaches seems to be very good. Since only two modes are excited during propagation, $n = 2$ and $n = 3$, we expect the beam to propagate mainly to the positive x direction. This can be verified by inspecting Figure 5(c) where the intensity evolution for a Gaussian beam with $W = 50$ is shown.

The existence of a pure trapped Bragg mode, as predicted in [21] for \mathcal{PT} -symmetric lattices, seems to be very rare and probably only achievable at the shallow potential approximation. So, even though the intensity pattern depicted in Figure 5(c) suggests a transparent medium, there is, in fact, another excited Bragg mode and, therefore, visible to the lattice (which reflects the field even with the lattice at the symmetry breaking point $b = 1$). We are now in a position to discuss an incident beam that excites Bragg modes with n negative. However, as demonstrated for \mathcal{PT} -symmetric lattices [21], when the photonic lattice is at the symmetry breaking point, the Bragg modes continuously absorb energy and diverge during propagation. Therefore, we expect our eleven-modes approach to become invalid for this regime, at least when z is large. To verify these claims, we present in Figure 6 the spectral evolution for a wavefield whose spectral amplitude $\psi_{-1}(0) = 1$ is initially populated while all others are zero. We clearly see that the amplitudes $\{\psi_1(z), \psi_2(z), \psi_3(z)\}$ grow indefinitely compared to the others. This implies that the medium is continuously giving energy to the field which becomes unbounded in amplitude. Figure 6(b) shows the power evolution predicted by (18) and we conclude that it describes very well the power evolution when compared to a Gaussian beam $\psi(x, 0) = \exp[-(1/2)(x/W)^2] \exp(-ix)$ with $W = 50$.

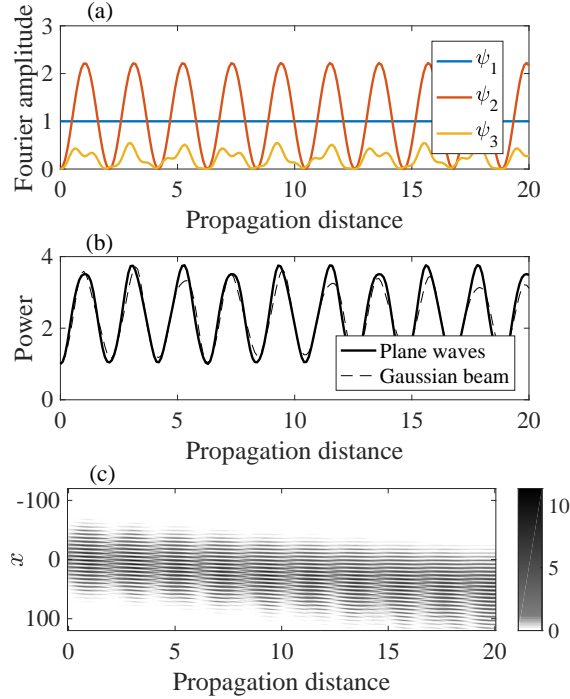


Figure 4: (a) Spectral amplitudes evolution with $\psi_1(0) = 1$ and all other modes empty to the lattice corresponding to Figures 1-3. (b) Power evolution calculated from the spectral amplitudes (solid line) and from the Gaussian beam (dashed line). (c) Intensity in the (x, z) plane for the Gaussian beam with $W = 50$.

Some others nonzero spectral amplitudes are shown in Figure 7 where, surprisingly, we see that the spectral amplitude ψ_0 does not grow indefinitely during propagation. It reproduces a pure Rabi-like profile exchanging energy periodically with the medium. This is the first time a stable Bragg mode is found when the incident beam is excited with n negative.

5. Conclusions

We have studied Bragg oscillations in a non- \mathcal{PT} -symmetric photonic lattice. It is shown that a nontrivial dynamics with asymmetric energy exchange between Bragg modes takes place during propagation of the wavefield. Depending on the incident angle, Rabi-like oscillations are indeed achievable in photonic lattices. The trapping of a pure Bragg mode in the more general context of a lattice with a non-vanishing amplitude was not observable even with the lattice at the symmetry breaking point. We have also found evidence of stable Fourier spectra evolution even if the incident beam has excited Bragg modes with n negative, that is, travelling in the negative x direction. This is the first time, to our knowledge, that a stable Fourier amplitude evolution is present in this configuration.

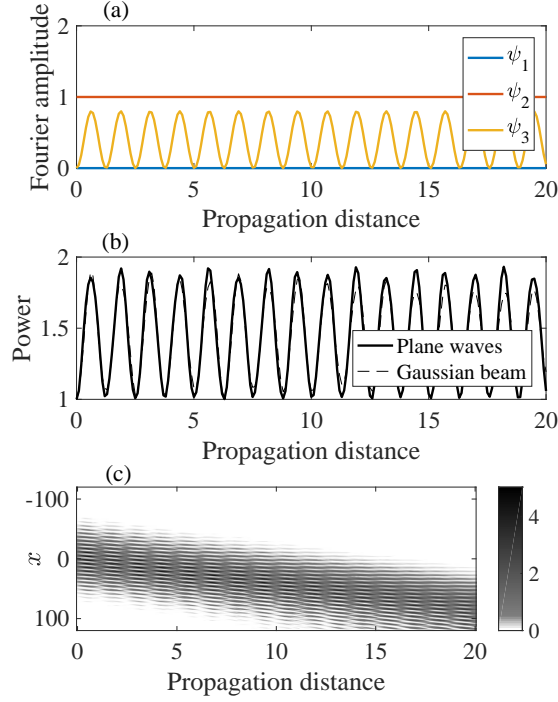


Figure 5: (a) Spectral amplitudes evolution with $\psi_2(0) = 1$ and all other modes empty to the lattice corresponding to Figures 1-3. (b) Power evolution calculated from the spectral amplitudes (solid line) and from the Gaussian beam (dashed line). (c) Intensity in the (x, z) plane for the Gaussian beam with $W = 50$.

References

- [1] C. M. Bender, S. Boettcher, Physical Review Letters **80**, 5243 (1998).
- [2] C. M. Bender, Rep. Prog. Phys. **70**, 947 (2007).
- [3] C. M. Bender, S. Boettcher, P. N. Meisinger, J. of Mat. Phys. **40**, 2201 (1999).
- [4] C. M. Bender, D. C. Brody, . H. F. Jones, Am. J. Phys. **71**, 1095 (2003).
- [5] K. G. Makris, R. El-Ganainy, D. Christodoulides, Z. H. Musslimani, Phys. Rev. Lett. **100**, 103904 (2008).
- [6] A. Guo, G. Salamo, D. Duchesne, R. Morandotti, M. Volatier-Ravat, V. Aimez, F. Siviloglou, D. Christodoulides, Phys. Rev. Lett. **103**, 093902 (2009).
- [7] C. E. Rüter, K. G. Makris, R. El-Ganainy, D. N. Christodoulides, M. Segev, D. Kip, Nat. Phys. **6**, 192 (2010).
- [8] L. Feng, M. Ayache, J. Huang, Y.-L. Xu, M.-H. Lu, Y.-F. Chen, Y. Fainman, A. Scherer, Science **333**, 729 (2011).
- [9] J. Rubinstein, P. Sternberg, Q. Ma, Phys. Rev. Lett. **99**, 167003 (2007).
- [10] C. M. Bender, B. K. Berntson, D. Parker, E. Samuel, Am. J. Phys. **81**, 173 (2013).
- [11] A. Mostafazadeh, J. of Math. Phys. **43**, 205 (2002).
- [12] A. Mostafazadeh, J. of Math. Phys. **43**, 2814 (2002).
- [13] A. Mostafazadeh, Int. J. of Geom. Meth. in Mod. Phys. **7**, 1191 (2010).
- [14] A. Mostafazadeh, A. Batal, J. of Phys. A: Math. and Gen. **37**, 11645 (2004).
- [15] J. Yang, Opt. Lett. **42**, 4067 (2017).
- [16] V. S. Shchesnovich, S. Chávez-Cerda, Opt. Lett. **32**, 1920 (2007).

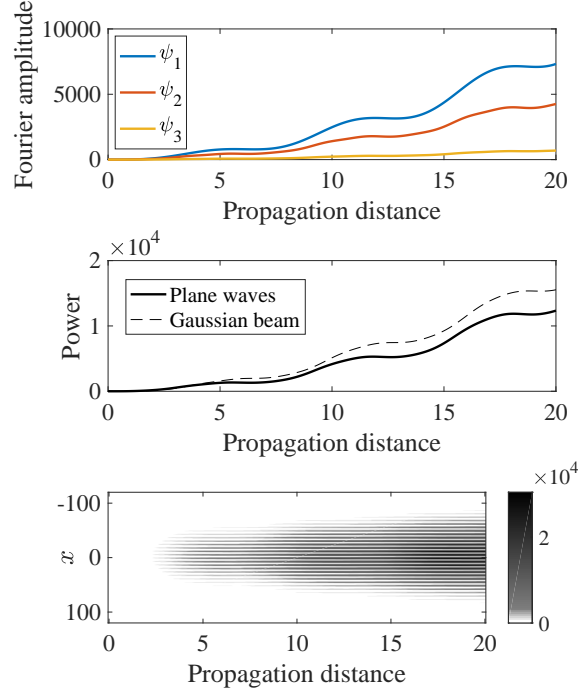


Figure 6: (a) Spectral amplitudes evolution with $\psi_{-1}(0) = 1$ and all other modes empty to the lattice corresponding to Figures 1-3. (b) Power evolution calculated from the spectral amplitudes (solid line) and from the Gaussian beam (dashed line). (c) Intensity in the (x, z) plane for the Gaussian beam with $W = 50$

- [17] K. Makris, D. Christodoulides, O. Peleg, M. Segev, D. Kip, Opt. Exp. **16**, 10309 (2008).
- [18] H. Trompeter, W. Krolikowski, D. N. Neshev, A. S. Desyatnikov, A. A. Sukhorukov, Y. S. Kivshar, T. Pertsch, U. Peschel, F. Lederer, Phys. Rev. Lett., **96**, 053903 (2006).
- [19] F. Dreisow, A. Szameit, M. Heinrich, T. Pertsch, S. Nolte, A. Tünnermann, S. Longhi, Phys. Rev. Lett. **102**, 076802 (2009).
- [20] S. Longhi, Phys. Rev. Lett. **103** (2009).
- [21] P. A. Brandão, S. B. Cavalcanti, Phys. Rev. A **96**, 053841 (2017).
- [22] P. A. Brandão, S. B. Cavalcanti, Opt. Commun. **400**, 34 (2017).
- [23] F. Cannata, G. Junker, J. Trost, Phys. Lett. A **246**, 219 (1998).
- [24] M.-A. Miri, M. Heinrich, D. N. Christodoulides, Phys. Rev. A **87**, 043819 (2013).
- [25] E. N. Tsoy, I. M. Allayarov, F. K. Abdullaev, Opt. Lett. **39**, 4215 (2014).
- [26] S. Nixon, J. Yang, Phys. Rev. A **93**, 031802 (2016).

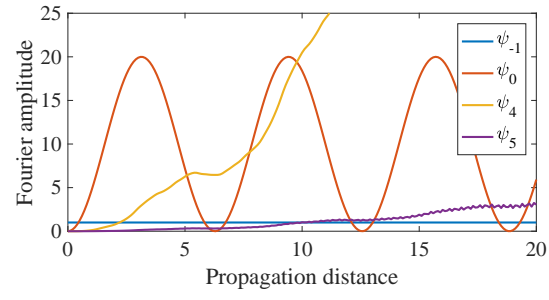


Figure 7: Fourier amplitude evolution for four modes with the system of Figure 6. One can clearly see that mode $\psi_0(z)$ is stable and oscillates in a Rabi-like fashion even though the beam is incident in the negative x direction.